Thermal dependence of the resistance of $TiN/Ti/HfO_2/Pt$ memristors

F. Jiménez-Molinos[1], G. Vinuesa[2], H. García[2], A. Tarre[3], A. Tamm[3], K. Kalam[3], K. Kukli[3], S. Dueñas[2], H. Castán[2], M.B. González[4], F. Campabadal[4], D. Maldonado[1], A. Cantudo[1], J.B. Roldán[1]

[1]Dep. Elec. y Tec. de Comp., Univ. de Granada, Avd. Fuentenueva s/n, 18071 Granada, Spain. Email: jmolinos@ugr.es
[2]Departamento de Electrónica, Universidad de Valladolid, Paseo de Belén 15, 47011 Valladolid, Spain.
[3]Institute of Physics, University of Tartu. Tartu, Estonia.
[4]Institut de Microelectrònica de Barcelona, IMB-CNM (CSIC), Carrer dels Til·lers s/n, 08193 Bellaterra, Spain.

2023 14th Spanish Conference on Electron Devices (CDE) | 979-8-3503-0240-0/23/$31.00 ©2023 IEEE | DOI: 10.1109/CDE58627.2023.10339514

***Abstract*—The thermal dependence of the resistance in the low resistance state of $TiN/Ti/HfO_2/Pt$ memristors has been experimentally studied. After modeling the measured I-V curves, the different resistive components (ohmic and non-linear) have been extracted and their thermal behavior estimated. Finally, the intrinsic series resistance linked to the metallic paths, contacts, and the remnants of the filament during resistive switching is also obtained at different temperatures. The results can be employed to propose physically-based models for circuit simulation.**

***Keywords*—memristor, thermal dependence, resistive switching**

I. Introduction

Memristors are subjected to a great interest, both by the industry and academy, due to their outstanding properties for data storage [1], neuromorphic applications [2], [3] and generation of true random numbers [1], among other applications. Resistive switching devices based on HfO_2 are a subset of memristors widely used thanks to the possibility of being programmed at different conductance levels (multilevel operation) [4], [5] and to the CMOS compatibility of their fabrication processes [6].

In resistive switching (RS) devices, the conductance can be switched, by the application of the appropriate electrical signals, between a high and a low level, although intermediate states can also be achieved, as previously mentioned. The latter device state is called high resistance state (HRS), while the former is known as the low resistance state (LRS). For devices with filamentary conduction, such as the ones studied here, the charge transport is due to a conductive filament (CF) formed in the dielectric (HfO_2) that shorts the two metallic electrodes. The disruption of this filament leads to the HRS in a process named reset, while the filament is rebuilt in the set process. A RS cycle includes set-reset-set processes, and it is usually performed under a ramped voltage signal. Due to the intrinsic stochastic nature of the involved switching mechanisms, the rebuilt CFs are different from the previous, and this leads to cycle-to-cycle variability [7].

In this work, we experimentally characterize and model the thermal dependance of the resistance in the LRS. During the experiments conducted in $TiN/Ti/HfO_2/Pt$ devices, the current is measured for a wide temperature range (90 K to 350 K), and the filament is not changed (RS cycling is not performed in this experiment). Therefore, the measured device resistance variations are linked to the thermal dependences of the conduction mechanisms, which are modeled and included in the conduction model. An accurate description of thermal effects is essential since the physical mechanisms behind RS are thermally activated [8].

On the other hand, according to some models [9], such as the Dynamic Memdiode Model [10], the device conductive path can be represented by a resistance in series with a non-linear component characterized by a potential barrier. The ohmic resistance has two components, one is fixed and does not change during cycling, while the other component is modified during the set and reset processes (as the non-linear component) [11]. The former is linked to the CF remnants and other conductive paths (such as electrodes and wires) and it is called series resistance (R_S) [11], [12]. This parameter can be experimentally extracted from I-V resistive switching characteristic curves under ramped voltage signals [11], [12]. In this work, this task has been performed at different temperatures in order to characterize the dependence of R_S on the temperature.

In section II, the device fabrication and the characterization setup are described. Section III presents the measured and modelled resistance as a function of temperature and the applied voltage, in the LRS (the device is not subjected to switching). Section IV deals with the series resistance extraction when the device is switched at different temperatures. Finally, the main conclusions are drawn in section V.

Authorized licensed use limited to: UNIVERSIDAD DE VALLADOLID. Downloaded on February 13,2024 at 15:40:37 UTC from IEEE Xplore. Restrictions apply.

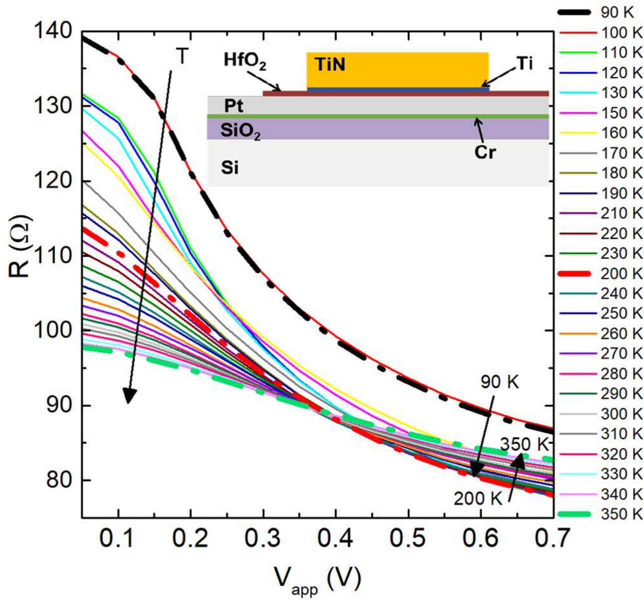

Fig. 1. Experimental resistance versus applied voltage measured from 90 K to 350 K (calculated as the applied voltage divided by the current). Note that different temperature dependences are observed at low and high voltages. Three representative curves have been highlighted (90 K, 200 K and 350 K). Inset: schematic representation of the device structure.

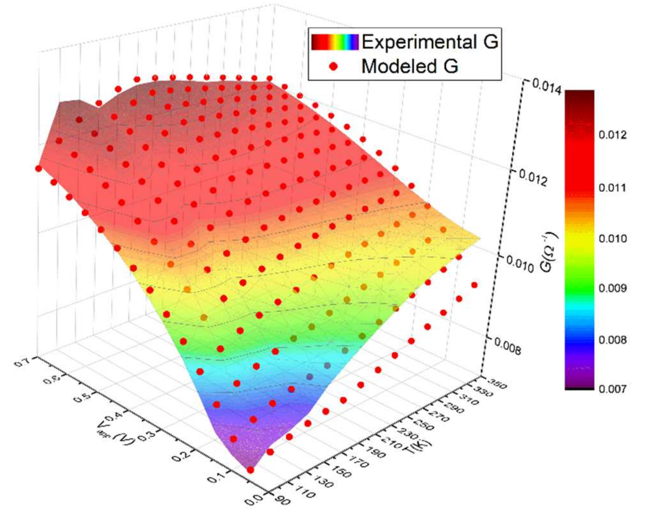

Fig. 2. Conductance versus applied voltage and temperature. The red dots correspond to the modeled conductance (calculated by simulation with LT-Spice using the model implemented in Ref. [9]), while the colored surface corresponds to the experimental data.

II. Fabrication and Experimental Setup

Cross-point TiN/Ti/HfO_2/Pt devices were fabricated on Si wafers with a thermally grown 200 nm SiO_2 layer. The bottom electrode consists of a 100 nm-thick Pt layer on a 5 nm Cr adhesion layer and the top electrode is a stack of 200 nm TiN on a 10 nm Ti layer. A 13 nm thick HfO_2 film was deposited by Atomic Layer Deposition (ALD) in a Picosun TM R-200 Advanced ALD System. The top electrode, which consisted of 200 nm thick TiN on a 10 nm Ti layer was deposited by magnetron sputtering and patterned by photolithography and lift-off. Finally, the electrical contact area to the bottom Pt electrode was defined by photolithography and dry etching of the HfO_2 layer. The resulting cross-point structures have an area of 60×60 μm^2. See inset in Fig. 1 for a schematic cross-section of the device and Refs. [9], [13], [14], for more information about the devices and fabrication process. The devices showed reproducible bipolar clockwise resistive switching [13].

The electrical measurements were carried out by a Hewlett-Packard Semiconductor Analyzer 4155B. Voltage bias was applied to the top electrode while the bottom electrode was grounded. The measurements were performed in a wide temperature range, from 77 K to 350K in an Oxford Instruments Cryostat DM1710 and monitored by an Oxford Instruments Temperature Controller ITC 503.

III. Thermal Dependence of the Resistance in the Low Resistance State

The I-V curves were measured in the low resistance state of the devices at different temperatures, with a maximum applied voltage of 0.7 V (lower than the reset voltage). Therefore, we can assume that the measured thermal dependence is not linked to a change in the filament configuration, but to the charge conduction thermal dependences. The filament had previously been formed with a set process at 77 K. Fig. 1 shows the experimental R-V curves (the resistance, R, is calculated as the applied voltage divided by the corresponding current). Different thermal effects have been obtained at the lowest and highest applied voltages, with a decreasing resistance dependence at the lowest voltages and more complex trends at the highest voltages (Fig. 1). For a fixed temperature, a non-ohmic behaviour is observed, with decreasing resistance as the applied voltage rises. This reduction is less noticeable for the highest temperatures. Fig. 2 shows the measured device conductance as a function of the applied voltage and device temperature. The filamentary conduction has been modeled and the thermal dependences correctly reproduced with a model that includes an ohmic resistance (R_{CF}) and a non-linear component (R_{NL}), both elements in series [9] (Fig. 3). The modeled conductance is also shown in Fig. 2. According to the previously mentioned dependences, it is expected that the relative importance of both components (R_{CF} and R_{NL}) changes under different temperature or applied voltage operation regimes.

From the fitting of the experimental I-V curves, both resistive components can be estimated. Fig. 4 shows the thermal dependences of R_{CF} and R_{NL} at different applied voltages. Both resistance components have been plotted versus the applied voltage for three representative temperatures in Fig. 5. Insets of Figs. 4 and 5 show the change in the relative importance of the ohmic component (R_{CF}) for the different voltage and temperature regimes. Note that the

Authorized licensed use limited to: UNIVERSIDAD DE VALLADOLID. Downloaded on February 13,2024 at 15:40:37 UTC from IEEE Xplore. Restrictions apply.

ohmic resistance (R_{CF}) is the most limiting component, except for the lowest applied voltages and temperatures.

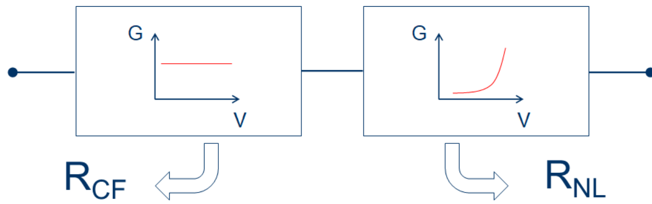

Fig. 3. Schematic representation of the LRS conduction model, with two series elements: an ohmic component (R_{CF}) and a non-linear part (R_{NL}). Each block includes different thermal dependences (see Ref. [9] for more details).

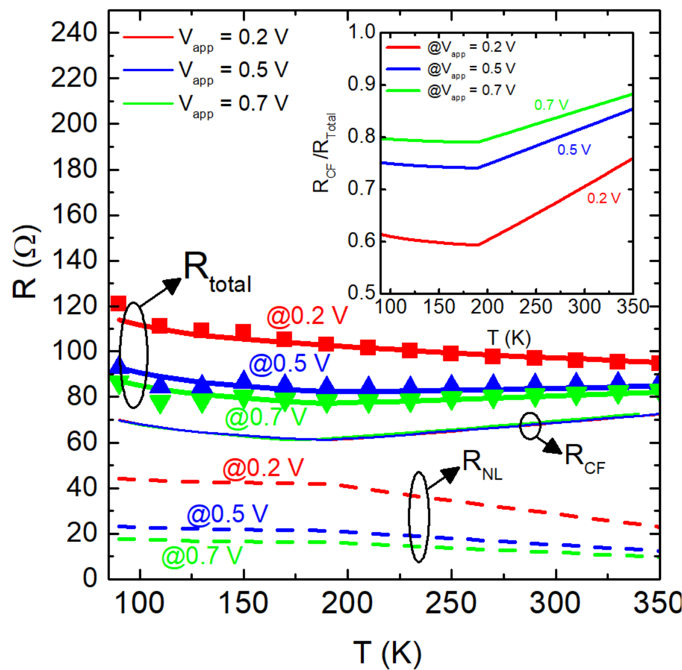

Fig. 4. Modeled conductive filament (solid line) and non-linear (dashed lines) resistance components versus temperature, for different applied voltages. The total modeled resistance (thicker solid line) is compared to the experimental total resistance (symbols). Inset: ratio between the ohmic and total resistances.

IV. Thermal Dependence of the Series Resistance

In a different experiment, RS cycles were performed at different temperatures, with 10 cycles for each temperature. Fig. 6 shows the measured I-V curves at 340 K. These curves can be plotted (inset in Fig. 6) using a corrected voltage given by the applied voltage minus the voltage drop in a series resistance, R_S [11]. This resistance is linked to wire conduction paths and contacts, in addition to the conductive filament remnants between different cycles [12]. While R_{CF} is the ohmic resistance component when the whole filament is formed (low resistance state), R_S includes only the part of the filament that remains basically unchanged (hardly changes during cycling).

Following the technique described in Refs. [11], [12], R_S has been estimated. The results are presented in Fig. 7. Note that the values of R_S are lower than those of R_{CF} (Fig. 4) because the latter correspond to a longer and completely formed filament in the LRS, while R_S includes a shorter portion of the CF. However, despite the variability of the estimated R_S values (Fig. 7) due to cycling, it is noticeable that the thermal dependence is quite similar for both resistances (R_{CF} and R_S, Figs. 4 and 7).

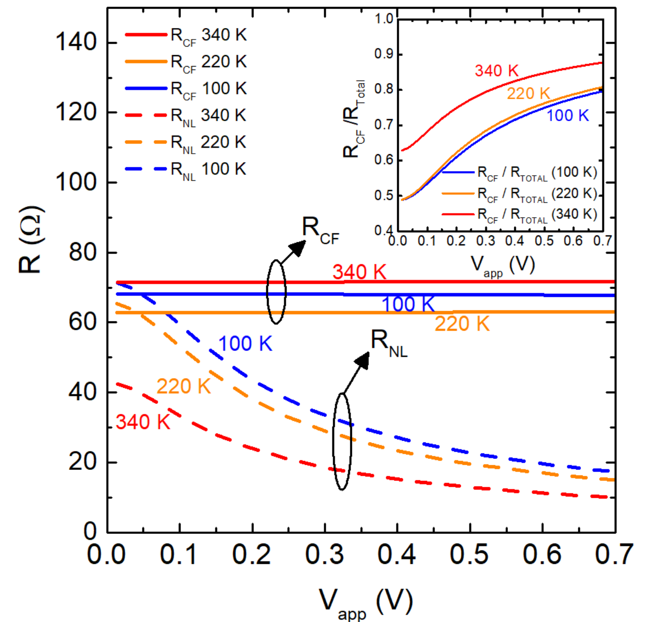

Fig. 5. Modeled conductive filament (solid line) and non-linear (dashed lines) resistance components versus applied voltage, for different temperatures. Inset: ratio between the ohmic and total resistances.

V. Conclusions

The thermal dependence of the resistance in the low resistance state of TiN/Ti/HfO_2/Pt resistive switching devices has been measured and modeled. The model includes two different resistive components (ohmic and non-linear) and their respective thermal dependences. By means of fitting the experimental R(V, T) data, the two resistance components are estimated and their relative weight plotted versus voltage and temperature. In addition, resistive switching cycles have been performed at different temperatures. The ohmic series resistance due to the wires and filament remnants that remain unchanged during cycling has been estimated for the measure temperatures. Finally, it should be noticed that the thermal dependences of both resistances (R_{CF} and R_S) obtained from both experiments are similar.

Authorized licensed use limited to: UNIVERSIDAD DE VALLADOLID. Downloaded on February 13,2024 at 15:40:37 UTC from IEEE Xplore. Restrictions apply.

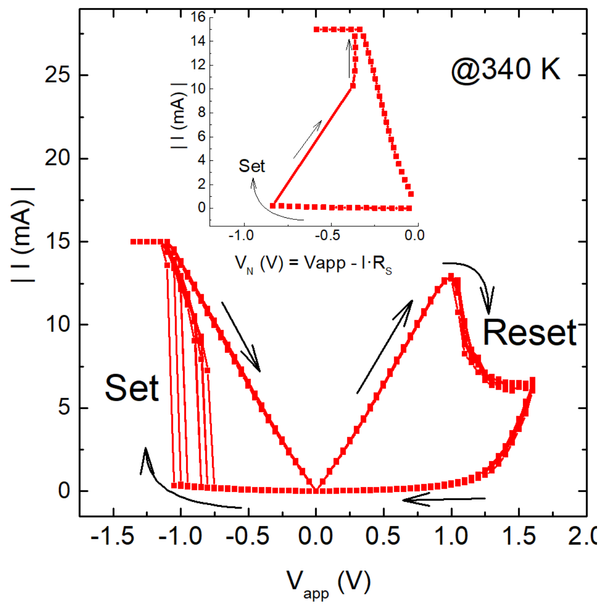

Fig. 6. Ten resistive switching cycles measured at 340 K. The inset shows the measured current versus the corrected voltage given by the applied voltage minus the voltage drop in the series resistance ($R_s = 51\ \Omega$), calculated following the methodology given in Refs. [11], [12] (for the 10th cycle).

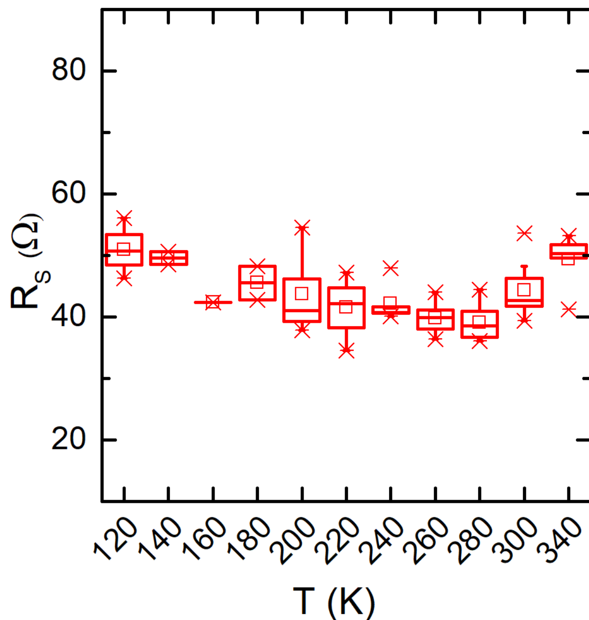

Fig. 7. Boxplot of the extracted serial resistance, R_S, at several temperatures. R_S is obtained following the methodology described in Refs. [11], [12].

ACKNOWLEDGMENT

This research was supported by the project B-TIC-624-UGR20 funded by the Consejería de Conocimiento, Investigación y Universidad, Junta de Andalucía (Spain) and the FEDER program. The study was also supported by the European Regional Development Fund project "Emerging orders in quantum and nanomaterials" (TK134), and the Estonian Research Agency (PRG753). M.B.G acknowledges the Ramón y Cajal grant No. RYC2020-030150-I.

REFERENCES

[1] M. Lanza et al., "Memristive technologies for data storage, computation, encryption, and radio-frequency communication", Science, vol. 376, eabj9979, 2022, doi: 10.1126/science.abj9979

[2] D. Florini et al., "A Hybrid CMOS-Memristor Spiking Neural Network Supporting Multiple Learning Rules", IEEE Transactions on Neural Networks and Learning Systems, pp. 1-13, 2022, doi: 10.1109/TNNLS.2022.3202501

[3] K. Zhu et al., "Hybrid 2D/CMOS microchips for memristive applications," Nature, in press, 2023, doi: 10.1038/s41586-023-05973-1.

[4] S. Poblador, M.B. González and F. Campabadal, "Investigation of the multilevel capability of TiN/Ti/HfO_2/W resistive switching devices by sweep and pulse programming", Micr.Eng. vol. 187-188, p. 148, 2018, doi: 10.1016/j.mee.2017.11.007

[5] H. García, O.G. Ossorio, S. Dueñas and H. Castán, "Controlling the intermediate conductance states in RRAM devices for synaptic applications", Micr. Eng. vol. 215, p. 110984, 2019, doi: 10.1016/j.mee.2019.110984

[6] E. Pérez et al., "Parameter Extraction Methods for Assessing Device-to-Device and Cycle-to-Cycle Variability of Memristive Devices at Wafer Scale," in IEEE Transactions on Electron Devices, vol. 70, pp. 360-365, 2023, doi: 10.1109/TED.2022.3224886.

[7] J. B. Roldán et al., "Variability in resistive memories", in press, doi: 10.1002/aisy.202200338

[8] J.B. Roldán et al., "On the thermal models for resistive random access memory circuit simulation", Nanomaterials, 11, 1061, 2021, doi: 10.3390/nano11051261

[9] F. Jiménez-Molinos et al., "Thermal effects on TiN/Ti/HfO_2/Pt memristors charge conduction", J. Appl. Phys., vol. 132, 194501, 2022, doi: 10.1063/5.0104890

[10] E. Miranda and J. Suñé, "Memristive State Equation for Bipolar Resistive Switching Devices Based on a Dynamic Balance Model and Its Equivalent Circuit Representation", IEEE Transactions on Nanotechnology, vol. 19, pp. 837-840, 2020, doi: 10.1109/TNANO.2020.3039391

[11] F.L. Aguirre, J. Suñé and E. Miranda, "SPICE Implementation of the Dynamic Memdiode Model for Bipolar Resistive Switching Devices", Micromachines, vol. 13, p. 330, 2022, doi: 10.3390/mi13020330

[12] D. Maldonado et al, "Experimental study of the series resistance effect and its impact on the compact modeling of the conduction characteristics of HfO_2-based resistive switching memories", Journal of Applied Physics, vol. 130, 054503, 2021, doi: 10.1063/5.0055982.

[13] G. Vinuesa et al., "Effect of dielectric thickness on resistive switching polarity in TiN/Ti/HfO_2/Pt stacks", "Electronics, vol. 11, p. 479, 2022, doi: 10.3390/electronics11030479

[14] K. Kukli, M. Ritala, T. Sajavaara, J. Keinonen and M. Leskelä, "Atomic Layer Deposition of Hafnium Dioxide Thin Films from Hafnium Tetrakis(ethylmethylamide) and Water", Chemical Vapor Deposition, vol. 8, pp. 199-204, 2002, doi: 10.1002/1521-3862(20020903)8:5<199::AID-CVDE199>3.0.CO;2-U

Authorized licensed use limited to: UNIVERSIDAD DE VALLADOLID. Downloaded on February 13,2024 at 15:40:37 UTC from IEEE Xplore. Restrictions apply.